

Photodissociation of Nitromethane using TOF Spectroscopy

A.Guerrero¹, C.Cisneros¹, I.Álvarez¹, E. Prieto¹, D.Martínez²

¹(Institute of Physical Sciences, UNAM., México)
²(Max Planck Institute for Nuclear Physics, Germany)
alfonsog@icf.unam.mx

ABSTRACT: We carry out experiments on the fragmentation of nitromethane by multiphoton absorption at the wavelength 266 nm. This was conducted in a reflectron (Jordan), modified in the laboratory. Due to the large number of fragments, special care has been taken into the calibration of the system, in the simultaneity between the laser pulse and the sample, and the associated electronics to ensure that produced fragment spectra arise from the interaction laser-sample. We emphasize the next aspects of the method:

- Simple design for introducing a gas sample at laser interaction region to facilitate the cluster formation
- Astonishing number of fragments and cluster formation are produced by multiphoton absorption.

KEYWORDS -Clusters, Multiphoton absorption, Nitromethane Photo dissociation, TOF mass spectrometry;

I. INTRODUCTION

The method of time-of-flight spectrometry has evolved since its practical implementation by Wiley and McLaren in 1955[1], introducing new sources of ionization, improving the resolution and using the new generations of more sensitive detectors.

The photofragments spectra of nitromethane multiphoton absorption were obtained from a high-resolution time of flight mass spectrometer, reflectron (R-TOF) (Fig.1). It is a commercial spectrometer (Jordan TOF Products Inc) modified in the laboratory and coupled to a vacuum chamber with a 60 cm diameter, housing the interaction zone where are generated the fragmented ions to be analyzed according to their mass to charge ratio (m/z). The essential components are the ion source, the laser and the sample, the acceleration system to provide uniform velocities to the ions within the field free region, and a suitable fast electronic, associated to the detection system. Basic design and components are shown in the diagram of the TOF. The uncertainty originated in the ion formation due to spatial distribution of the molecules in the region of interaction between the electrically polarized electrodes is minimized from the second electrode before the ions enter to the drift region. Since the trajectory is fixed, we can measure the velocity v of the fragmented charged ions ($v=(2ZeV/m)^{1/2}$, with m the ion mass, e electron charge and V the acceleration voltage). In addition, we can use the system in linear mode or as Reflectron and use the electrostatic mirror to compensate differences in the initial velocities at the exit from the source before entering into the drift region. As an example, the velocities of some fragments with different masses and acceleration voltage are presented below.

Velocities at 1 keV: 1 amu: H^+ : 4.38×10^7 cm/s

2 amu: H_2^+ : 3.09×10^7 cm/s $\Delta(1,2) = 1.29 \times 10^7$ cm/s

Velocities at 1.5 keV : 1 amu: H^+ : 5.36×10^7 cm/s

2 amu: H_2^+ : 3.79×10^7 cm/s $\Delta(1,2) = 1.57 \times 10^7$ cm/s

323 amu: $(M)_5H_2O^+$: 2.98×10^6 cm/s

367 amu: $(M)_6H^+$: 2.8×10^6 cm/s $\Delta(323,367) = 0.18 \times 10^6$ cm/s

Where M is the original molecule.

II. THE METHOD

2.1 The Ion Source

We used a pulsed valve and a skimmer to generate a supersonic molecular beam in a collision free system. Between the valve and the skimmer there is an extension with a conical termination, inside the chamber, that allows the gas to expand adiabatically closer to the skimmer. There is a 10 mm gap between the end of the extension and the entrance of the skimmer. As radiation source a 30 Hz Nd:Yag laser was used from Spectra Physics with temporal pulses of 4 to 5 ns at 266 nm wavelength. The manufacturer sets the pulse duration. The laser radiation (with a Gaussian profile and vertically polarized) was focused into the interaction region using a 15 cm focal length UV-lens. The diameter of the spot at the focal point was 80.0 μ m. Radiation intensities between 10^9 and 10^{10} $W \cdot cm^{-2}$ were achieved under these experimental conditions. To reach the adequate interaction laser/molecule it was necessary to synchronize the time between the laser shot and the time of travel of the sample to arrive simultaneously at the center of the interaction region.

The synchronization was attained opening the valve in advance to the emission of the laser pulse, this takes into consideration the time of arrival of the molecular cloud at the outlet of the valve towards the center of the region of interaction with the laser beam. The pulsed valve can be controlled manually to obtain the maximum signal, however the best way to synchronize the laser shot and the sample plume at the center of the interaction region is to use a special pulse delay device designed for that purpose. When the laser generates a pulse of light, the control electronics simultaneously provide a pulse of voltage TTL. This TTL signal is introduced in the retarding electronic device generating a similar pulse but retarded. This pulse is used to produce a voltage which opens the pulsed valve before a second light pulse out of the laser and interacts with the sample plume in the interaction region. If t_d is the time of the open valve to obtain the optimal synchrony between the laser pulse and the molecular sample, then its value: $t_d = (1/\nu) - t_1$; where ν is the laser frequency and t_1 the delayed time compared to the TTL previous signal. See Fig.2.

2.2 The Sample

The study of Nitromethane was chosen due to its great interest in atmospheric and interstellar chemistry [2] as well as being an efficient energy source [3,4,5]. It is a complex molecule that has been studied with different experimental techniques [6,7,8,9], in particular, the one used in the present work is the multiphotonic ionization / dissociation induced by laser absorption at 266 nm wavelength. Multiphoton spectroscopy is an excellent method since it is possible to access high-energy molecular states being able to analyze the dissociation and ionization of large molecules.

A sample of liquid nitromethane was purchased from Sigma-Aldrich (purity ~99%). The nitromethane vapor pressure was 3.7 kPa (27.75 torr) at 20°C. The sample was heated at a constant temperature of 28°C and introduced in gas phase into the ionization chamber by a pulsed valve. The pulsed valve has an extension with a conical termination inside the chamber that allows the gas adiabatically to expand closer to the skimmer to generate a supersonic molecular beam. Being a supersonic beam velocity and considering the distance traveled of ~ 15 cm from valve to center of the interaction region, the time in advance of the opening should be of the order of some milliseconds. The final tuning is adjusted in the device of delay until the best signal is obtained.

The nitromethane gas and laser pulse interact at 90° (Fig. 3). This region was located between two electrically polarized electrodes separated by 6 mm and with a circular mesh of 90% transparency and a 1 cm diameter. The positive fragments formed at the nanosecond laser pulse were accelerated to the free field region of the R-TOF mass spectrometer by applying an extraction voltage to the electrodes, in the present case it was 1.5 keV.

Finally, after the ions pass the drift zone, they are directed to the detector, which is a dual microchannel plate (Chevron). The signals from the microchannel plate are routed to a fast preamplifier VT 120 and analyzed by a multichannel analyzer (both Ametek/ ORTEC). A computer collects and processes the data according to the arrival time of the fragments and their charge/mass relation. While the ions are produced the operating pressure is 2×10^{-6} torr with an open valve (175 μ s), the base pressure is 9×10^{-8} torr reached by the operation of two turbo molecular pumps (models Navigator 301 and 551 Agilent). Once the fragment spectra were obtained it is necessary to identify the correspondent peak to a specific fragment. To do this it is needed to calibrate the system. In order to achieve that, when the molecular sample arrives at the center of the ion source and is ionized from the laser, the charged ions feel the extraction voltage and the cations are accelerated toward the drift region. The acquired kinetic energy will be proportional to the potential difference (V) between the electrodes: $\frac{1}{2}mv^2 = qV$ and $v = (2qV/m)^{1/2}$. Since $v = L/t$ where L is the drift region length and t is the flight time: $t = L(m/2qV)^{1/2}$. The difference transit time for masses m_1 and m_2 can be expressed as follows: $\Delta t = (L m_1^{1/2} - L m_2^{1/2}) / (2qV)^{1/2}$

For two ions with the same charge and kinetic energy, but different mass $m_1v_1^2 = m_2v_2^2$, if L is the drift length, we have $t_1/m_1^{1/2} = t_2/m_2^{1/2}$, and knowing the time for one fragment, it is possible convert the time of flight for the other fragments and generate a mass spectrum.

As an example, the spectrum of the nitromethane fragments obtained in the interaction with laser Nd: YAG at 266 nm wavelength and 4 ns temporal width is shown (Fig. 4). Table 1 shows some of the fragments identified using the method described and Table 2 with the clusters identified.

2.3 Calibration

With the calculated m/z value and flight times, a calibration curve is constructed from which the equation that conforms to the values of the masses is obtained. Figure 5 shows the calibration curve for nitromethane at 266 nm and the related equation.

It is interesting to notice that the spectra in figures 4,5 shows fragments with masses greater than 61, which corresponds to the mass of the molecular ion. In Table I are fragments containing C₂ and C₃. This is due to the presence of clusters. Pulsed valve, tube extension and the skimmer favor the formation of aggregates or clusters,

which, in turn originate the fragments with C_2 , C_3 , C_2H_2 , C_3 and so on. The presence of clusters and the duration of the laser pulse produce a large number of fragments [8,9].

2.4 The Electronics for the Time Flight

The important aspect in the TOF experiments are the times involved in the different steps in the processes. The time interval of the laser shot for a frequency 30 Hz will be ~33 milliseconds, the aperture of the valve, in the range of microseconds (~175 μ s). The molecular beam is supersonic (~ 10^2 m/s). The temporal width of the laser is in the nanosecond range 10^{-9} s. The molecular reaction, in the case of nitromethane 10^{-12} s.

The electronics of the detection system allow practically any ions to be recorded, since it is the time difference that differentiates the masses. In the multichannel system (EASY MCS Ortec/Ametek), the temporal scan can be done from a very short time (400 ns) to a very long time (2.7 years) using around 65 thousand channels. The detector is a microchannel plate (MCP), which receives the signal of ions when hitting the detector surface and the small electric charge which is produced goes to the preamplifier and converted to a voltage pulse. The response is of the order of nanoseconds. Figure 1 also shows the electronic configuration of the experimental system.

2.5 The Resolution

As an example, consider the velocities for the single charge fragments with amu 1 and amu 2 at 1 keV acceleration potential and the time of travel one meter to the detector, we have:

For 1 amu, $v = 4.38 \times 10^7$ cm/s the time to travel 1m is: $t = 2.28 \times 10^{-6}$ s

For 2 amu $v = 3.09 \times 10^7$ cm/s the time to travel 1m is: $t = 3.23 \times 10^{-6}$ s

The time interval for that masses (1,2) will be: $\Delta(1,2) = 0.95 \times 10^{-6}$ s

The difference in time of arrival to the detector for ions with 1 amu and 2 amu is ~ 10^{-6} s and the detection time is 10^{-9} s. The microchannel plate is therefore able to differentiate the times of arrival of each ion. On the other hand, the electronic response time is 10^{-12} s. So, is how by rapidly transforming the current generated by the ions to analog and finally to digital, excellent resolution is guaranteed.

To show this consider the difference in transit time Δt for two masses m_1 and m_2 :

$$\Delta t = (Lm_1^{1/2} - Lm_2^{1/2}) / (2qV)^{1/2}$$

This can be approximated [$(\Delta t)^2 > 0$] by $m/\Delta m = t/2\Delta t$ where t corresponds to the time of flight of the selected ion and Δt corresponds to the width of the signal at half the maximum (FWHM). The Figure 6 shows some of the resolution values calculated for different masses.

With the characteristics of the pulsed laser (30 Hz), the synchrony between opening of the valve and the pulses of the laser radiation guarantees that different masses-ionized fragments will be detected without overlap and will be processed equally due to the fast electronics.

III. FIGURES AND TABLES

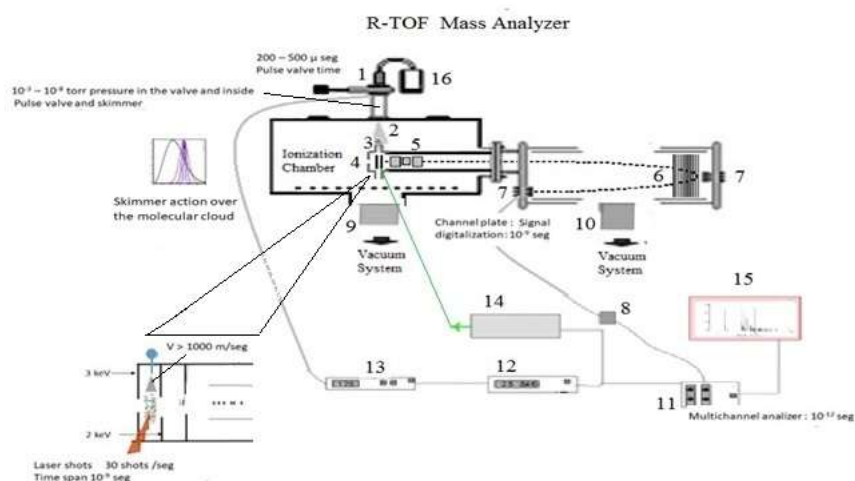


Figure 1. Diagram of the experimental system. 1.Pulsed valve. 2.Extension. 3.Skimmer. 4.Interaction region: polarized electrodes 5. Electrostatic focus & deflection plates 6. Electrostatic mirror, 7. Detector: microchannel plate of the R-TOF 8. Preamplifier. 9 &10. Vacuum system, 11. ORTEC picoammeter, 12. Electronic for the control the time for the valve and the laser. 13 Control of the valve aperture 14 laser, 15. Data processing. 16. Sample container

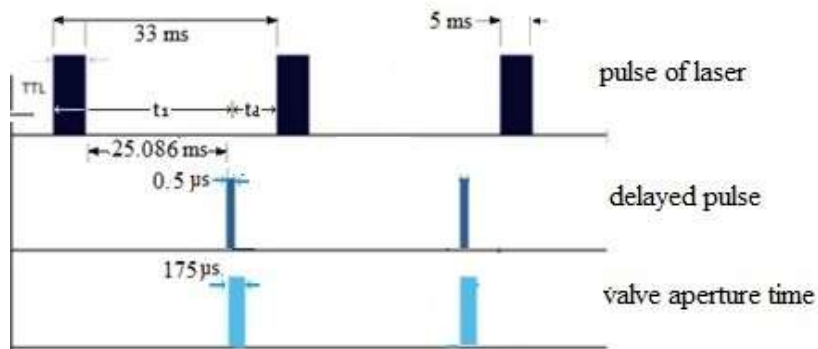


Figure 2. Diagram of the synchronization of the TTL pulses, delayed and opening of the valve.

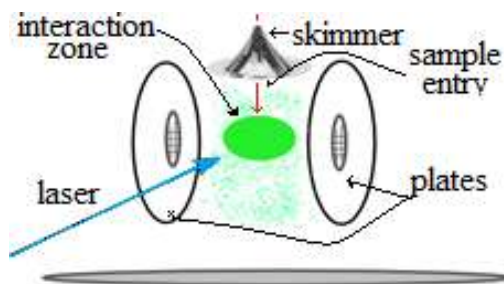


Fig.3 Laser-sample interaction

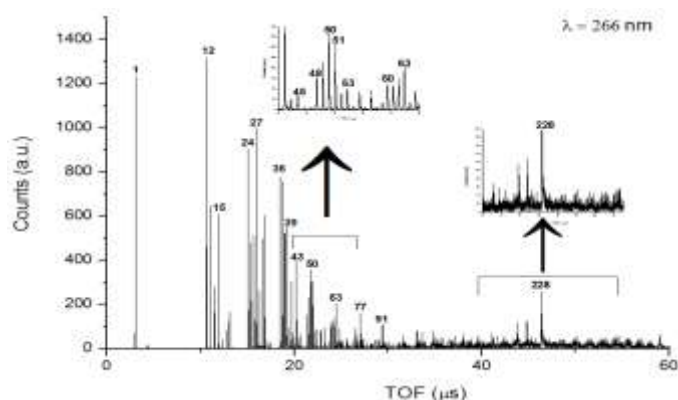


Figure 4.- Flight time spectrum of nitromethane at 266 nm and an irradiation power of 1.24×10^{10} W/cm².

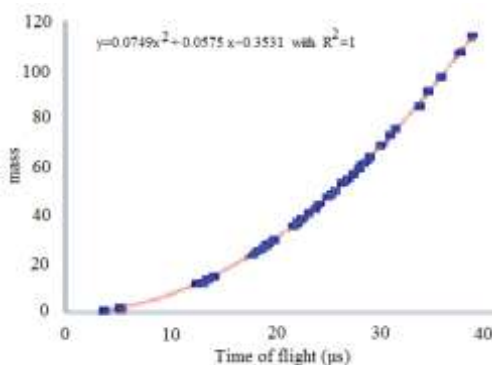


Figure 5.- Calibration curve for nitromethane ions formed by multi-photon absorption at 266 nm

Table 1

ION	m/z	ION	m/z	ION	m/z	ION	m/z
H ⁺	1	C ₂ ⁺	24	C ₃ ⁺	36	CO ₂ H ⁺ CH ₃ NO ⁺	- 45
H ₂ ⁺	2	C ₂ H ⁺	25	C ₃ H ⁺	37	CO ₂ H ₂ ⁺ NO ₂ ⁺	- 46
C ⁺	12	C ₂ H ₂ ⁺	26	C ₃ H ₂ ⁺	38	C ₂ HNO ⁺	55
CH ⁺	13	C ₂ H ₃ ⁺	27	C ₃ H ₃ ⁺	39	C ₂ H ₂ NO ⁺ C ₂ O ₂ ⁺	- 56
CH ₂ ⁺	14	CNH ₂ ⁺ CO ⁺	- 28	C ₂ O ⁺	40	C ₂ H ₃ NO ⁺ C ₂ O ₂ H ⁺	- 57
CH ₃ ⁺	15	CNH ₃ ⁺ HCO ⁺	- 29	C ₂ HO ⁺	41	CNO ₂ ⁺	58
O ⁺ -CH ₄ ⁺	16	NO ⁺ H ₂ CO ⁺	- 30	CNO ⁺ C ₂ H ₂ O ⁺	- 42	CHNO ₂ ⁺	59
OH ⁺ -CH ₅ ⁺	17	COH ₃ ⁺ NOH ⁺	- 31	CHNO ⁺ C ₂ H ₃ O ⁺	- 43	CH ₂ NO ₂ ⁺	60
H ₂ O ⁺ -CH ₆ ⁺	18	NOH ₂ ⁺	32	CH ₂ NO ⁺	44	CH ₃ NO ₂ ⁺	61

Table 1. Some of the fragments identified by the method described in the text.

Table 2

Cluster	m/z	Cluster	m/z
(NM)H	62*	(NM) ₂ [C ₂ H ₃ NO-C ₂ O ₂ H]	179
(NM)H ₂	63	(NM) ₃	183*
(NM)CH	74	(NM) ₃ CH ₃	198*
(NM)O	77	(NM) ₃ [CNH ₃ -HCO]	212
(NM)NO	91*	(NM) ₃ CH ₃ NO	228*
(NM) ₂ NO	152*	(NM) ₅ H ₂ O	323
(NM) ₂ O ₂ H	155*	(NM) ₆ H	367*

Table 2. Clusters formed with nitromethane The asterisks indicate clusters also identified by Ferreira [10].

IV. CONCLUSION

Using a R-TOF and the multiphoton absorption technique we are able to detect the copious fragmentation of a sample of nitromethane. The experimental design allows cluster formation and these to the fragmentation. The experimental parts, as the introduction of the sample, the synchrony of the sample and laser shots, the calibration of the spectrum and the influence in the design of the introduction of the sample and all the associated electronics are emphasized.

V. Acknowledgements

This work was supported by DGAPA PAPIIT grants No. IN104423

REFERENCES

- [1]. Wiley, W. C. and McLaren, I. H. Time-of-Flight Mass Spectrometer with Improved Resolution, *Rev. Sci. Instrum.* 26, 1150 (1955); <https://doi.org/10.1063/1.1715212>
- [2]. Schwind R., Sinrud J., Fuller C., Klassen M., Walker R. A. and Goldsmith F., Comparison of flame inception behavior of liquid nitromethane in inert and air environments, *Combustion and Flame* 241 (2022) 112101
- [3]. Vinogradov A., Nekipelov S.V., Pavlychev A., Boronov A. and Zhadenov A. V., X-ray absorption spectra of the nitromethane molecule CH₃NO₂, *Optics and Spectroscopy* · January 1992

- [4]. Bhowmick M., Nissen E.J. and Dana D. Dlott, Detonation on a tabletop: Nitromethane with high time and space resolution, *J. Appl. Phys.* 124, 075901 (2018); <https://doi.org/10.1063/1.5043540>
- [5]. Shrestha K.P., Vin N., Herbinet O., Seidel L., Battin-Leclerc F., et al., Insights into nitromethane combustion from detailed kinetic modeling – Pyrolysis experiments in jet-stirred and flow reactors, *Fuel*, 2020, 261, pp.116349. hal id. 10.1016/j.fuel.2019.116349
- [6]. [Martínez D.](#), [Guerrero A.](#), [Prieto E.](#), [Álvarez I.](#), [Cisneros C.](#), Clusters formation and fragmentation of nitromethane at 266 nm, *MethodsX*. 2020 May 1;7:100909.doi: 10.1016/j.mex.2020.100909
- [7]. [Guo Y.Q.](#), [Bhattacharya A.](#), [Bernstein E.R.](#), Photodissociation dynamics of nitromethane at 226 and 271 nm at both nanosecond and femtosecond time scales, *J Phys Chem A*. 2009. Jan 8;113(1):85-96. doi: 10.1021/jp806230p
- [8]. Scoles G. Editor and Bassi D., Atomic and Molecular Beam Methods, Udo Buck and Derek Laine Ass.Editors Chapter 3, section 323. *Oxford University Press* 1988
- [9]. Kaiser R.I. and Maksyutenko P., Novel Reaction Mechanisms Pathways in Electron. Induced Decomposition of Solid Nitromethane (CH₃NO₂) and D₃- Nitromethane (CD₃NO₂), *J. Phys. Chem. C* 2015, 14653-14668
- [10]. Ferreira da Silva F., Ptasinska S., Denifl S., Gschliesser D., Postler J., Matias C., Märk T. D., Limão-Vieira P. and Scheier P.; Electron interaction with nitromethane embedded in helium droplets: Attachment and ionization measurements; *J. Chem. Phys.* 135, 174504 (2011)